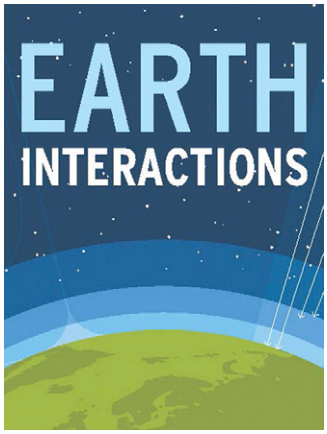


Copyright © 2016, Paper 20-018; 76451 words, 15 Figures, 0 Animations, 3 Tables.
http://EarthInteractions.org

Towards an Understanding of the Twentieth-Century Cooling Trend in the Southeastern United States: Biogeophysical Impacts of Land-Use Change

W. L. Ellenburg[a]

Earth System Science Center, University of Alabama in Huntsville, Huntsville, Alabama

R. T. McNider

Department of Atmospheric Science, University of Alabama in Huntsville, Huntsville, Alabama

J. F. Cruise

Earth System Science Center, University of Alabama in Huntsville, Huntsville, Alabama

John R. Christy

Earth System Science Center, University of Alabama in Huntsville, Huntsville, Alabama

Received 22 June 2015; in final form 4 April 2016

[a] *Corresponding author address*: W. L. Ellenburg, Earth System Science Center, University of Alabama in Huntsville, 320 Sparkman Dr., Huntsville, AL 35805.
E-mail address: lee.ellenburg@uah.edu

DOI: 10.1175/EI-D-15-0038.1

ABSTRACT: This paper explores the link between the anomalous warming hole in the southeastern United States and a major land-use/land-cover (LULC) change in the region. Land surface and satellite observations were analyzed to estimate the net radiative forcing due to LULC change. Albedo and latent energy were specifically addressed for the dominant LULC change of agriculture to forests. It was assumed that in the energy-limited environment of the region, the partition of changes in available energy due to albedo will mostly impact the sensible heat. The results show that in the southeastern United States, for the period of 1920 to 1992, the changes in sensible (as a result of albedo) and latent energies are in direct competition with each other. In the spring and early summer months, the croplands are in peak production and the latent energy associated with their evapotranspiration (ET) is comparable to that of the forests so the decrease in radiation due to albedo dominates the signal. However, during the late summer and fall months, most major crops have matured, thus reducing their transpiration rate while forests (particularly evergreens) maintain their foliage and with their deep roots are able to continue to transpire as long as atmospheric conditions are favorable. This later influence of latent energy appears to more than offset the increased radiative forcing from the spring and early summer. Overall, a mean annual net radiative forcing resulting from a LULC change from cropland to forests was estimated to be $-1.06\,\mathrm{W\,m^{-2}}$ and thus a probable contribution to the ''warming hole'' over the Southeast during the majority of the twentieth century.

KEYWORDS: Physical meteorology and climatology; Climate change; Latent heating/cooling; Radiative forcing; Observational techniques and algorithms; Satellite observations; Surface observations; Applications; Land use

1. Introduction

The Fifth Assessment Report (AR5) of the Intergovernmental Panel on Climate Change (IPCC; Hartmann et al. 2013, their Figures 2.20–21) shows that over most of the world, gridded annual surface air temperatures have increased from 1901 to 2012. The record for the period displays three distinct temperature phases as shown in Figure 1 below. The first decades of the century were dominated by a rising trend where temperatures rose about 0.4°C that ended in about 1940. Then, until roughly 1975, a slight cooling trend resulting in a decline of approximately −0.1°C can be observed. In the last decades of the century, and continuing to the present, warming again dominates the signal. As a rule, the warming is greater over the higher latitudes, and more warming is observed over land than over water.

Various causes have been ascribed to the midcentury cooling trend including ''global dimming'' due to aerosols (Wild et al. 2007; Yu et al. 2014), volcanic eruptions (Meehl et al. 2004), and solar irradiance (Crowley 2000; Meehl et al. 2004). Meehl et al. (2004) employed global climate models to show that an additive effect of all of the enumerated causes is necessary to simulate the record. Recently, authors have pointed to a slowing of the Atlantic Ocean overturning circulation as a further causal mechanism (Rahmstorf et al. 2015).

The magnitude of the midcentury cooling trend is most striking over North America as compared to the other continents (Hartmann et al. 2013). However, this phenomenon does not appear to be evenly distributed over the whole of the region (Zhang et al. 2000; Portmann et al. 2009; Lawrence et al. 2012; Dobrowski et al.

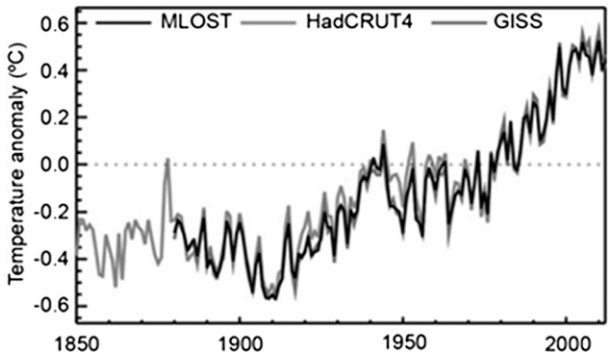


Figure 1. From **Hartman et al. (2013**, their Figure 2.20): Annual global-mean surface temperature anomalies relative to a 1961–90 climatology from the latest version of the three combined land surface air temperature and sea surface temperature datasets (HadCRUT4, GISS, and NCDC Merged Land–Ocean Surface Temperature analysis).

2013). For example, Zhang et al. (2000) demonstrated significant differences in temperature trends across Canada with a warming in the southern and western portions of the country and cooling in the Northeast. Similarly, several authors have identified significant spatial trends across the United States with reduced cooling (or even slight warming) in the western states and a cooling tendency in the central and eastern areas (Knappenberger et al. 2001; Dobrowski et al. 2013; Meehl et al. 2013). Of note, authors have pointed to significant "warming holes," that is, cooling trends over part or even most of the century in the upper midwestern, south-central, and southeastern United States (Pan et al. 2004; Kunkel et al. 2006; Meehl et al. 2012). Although the midwestern and south-central anomalies appear to have largely disappeared in the last 20 years of the last century, the southeastern warming hole has diminished in spatial scope but still persists today, located primarily over the states of Alabama and Mississippi. Figure 2 shows the National Climate Data Center's division temperature trend from 1985 to 2014. Though the latter quarter of the century exhibits a spatially consistent rising trend across the United States, the persistence of the cooling phenomenon over the Southeast induces the unique characteristic that the region exhibits a slight cooling trend over the entire twentieth century (see Figure 2).

The southeastern cooling episode exhibits several notable and unique features: its earlier onset, its persistence well into the twenty-first century (albeit at a smaller spatial scale), and, most notably, its decline in minimum as well as maximum temperatures (Knappenberger et al. 2001). The causes of the southeastern trend are thought to be fundamentally different than those associated with the midwestern and south-central trends (Portmann et al. 2009; Meehl et al. 2012; Rogers 2013). While no definitive cause has been identified for the persistence of this phenomenon, several theories have been advanced by climate scientists. These include "dimming" due to aerosols (Saxena and Yu 1998; Portmann et al. 2009; Leibensperger et al. 2012); increased cloudiness, precipitation, and soil moisture variability (Pan et al. 2004); variability of SST in the both the Atlantic and Pacific (Robinson 2002; Kunkel et al. 2006; Wang et al. 2009); and reduced sensible heat loss due to increased irrigation (Christy et al. 2006; Puma and Cook 2010).

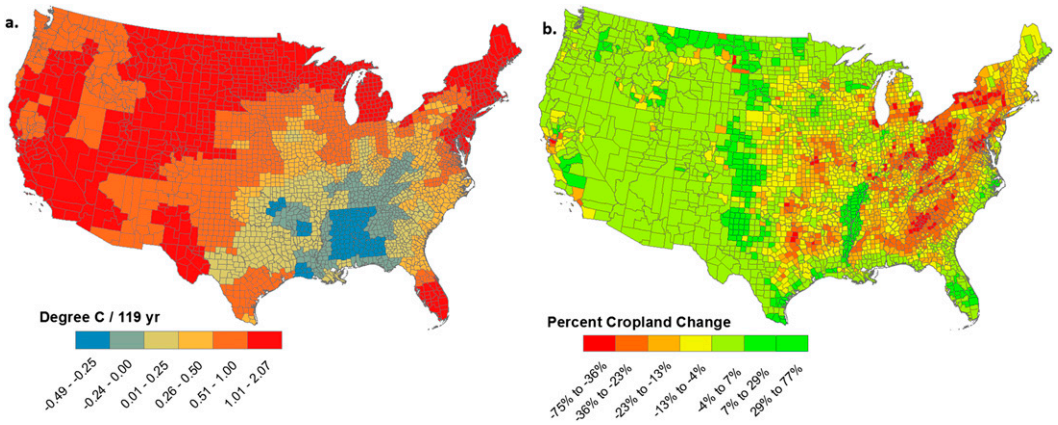


Figure 2. Conterminous U.S. (a) temperature trends from 1895 to 2014 and (b) cropland loss from a Southeast maximum in 1920 to 1992 (Waisanen and Bliss 2002).

In a comprehensive study of the southeastern United States, primarily the states of Mississippi, Alabama, and Georgia, Rogers (2013) found that 60% of the summer temperature variance was primarily described by soil moisture and cloud cover; however, all the predictor indices examined combined explained less than 38% of the annual and winter variance. Land-use/land-cover (LULC) change has been shown to alter cloudiness and potentially precipitation (McNider et al. 1994; Wetzel and Chang 1987) so that some part of the soil moisture and cloudiness relationship found by Rogers (2013) may be an indirect effect of LULC change.

Coincident with the past century's warming hole, the southeastern United States experienced a major LULC change. While the region was a major agricultural producer at the turn of the twentieth century, the 60 years that followed saw a drastic reduction of cropland. The rain-fed agricultural system in place was no match for the irrigating farmers in the west or the midwestern farms that are largely insulated from drought by their deep water-holding soils. By 1980, western irrigation and improvements in transportation had largely displaced the rain-fed systems of the east, and as a result southeastern agriculture declined precipitously. In Alabama, planted acres of corn and cotton have decreased by 90% over the past century (Census of Agriculture, National Agricultural Statistical Service, www.nass.usda.gov). On average, the Southeast as a whole lost 45% of agricultural land since 1920 (Waisanen and Bliss 2002), with Florida as the only state with a net gain. In addition to the loss of cropland, forests in the Southeast were rebounding from the significant cutting that went on from the 1880s to 1920s (Bronaugh 2012).

As seen in Figure 2, the loss of agriculture is not unique to only the Southeast; indeed, most the eastern United States experienced notable cropland loss. However, an important aspect of that land-cover change is unique to the southeastern region. Urban and suburban areas in the Northeast grew rapidly, filling the gap where agricultural land once existed. In the Southeast, population actually declined during this period in most of the agricultural counties (Waisanen and Bliss 2002).

Additionally, since the Northeast was developed earlier, it rebounded from logging earlier. The Southeast continued logging its natural forests (steep terrain and coastal plains) into the 1920s, exporting lumber to the rest of the United States and the world before reforestation started (Bronaugh 2012). Meanwhile, as rural economies, dependent on local and regional agriculture, descended into poverty, the Conservation Reserve Program (CRP) and timber plantations filled the vacuum of fallow land. The Southeast, now known as the world's ''wood basket'' is responsible for 60% of the national timber industry (Prestemon and Abt 2002) and produces more wood products than any other nation, except the United States as a whole. The USGS Land Cover Trends Project (Napton et al. 2009) found that most of the land-cover change over the last quarter of the century in the Southeast was due to forest harvesting and regrowth, agricultural abandonment, and development.

Given the importance of LULC on the coupled land–atmosphere system (Pielke et al. 2002), it is possible that the major cultural LULC shift over the past century in the southeastern United States could have had a significant influence on the climate of the region, explaining, in part, the temperature anomalies that are inconsistent with global and national trends. Both observations and models have been implemented to study the impact of land-use and land-cover change on both the global and regional scales (Pielke et al. 2002; Trail et al. 2013; Christy et al. 2006; Shi et al. 2014; Mahmood et al. 2014; Beltrán-Przekurat et al. 2012; Baldocchi and Ma 2013; Kalnay and Cai 2003; Fall et al. 2010). In particular the Land-Use and Climate, Identification of Robust Impacts (LUCID) program has focused on land-cover impacts at global and regional scales (Pitman et al. 2009; de Noblet-Ducoudré et al. 2012; Boisier et al. 2014), and Findell et al. (2007) provides a conceptual framework of the physical process involved when analyzing the impacts of LULC change. While model results have been mixed, the data do tend to show that at the regional scale, land-use change impacts can be significant. In fact, research synthesis of land-cover impacts on climate have been produced, and repeated calls for further research into this issue have been made (Mahmood et al. 2010, 2014; Pielke et al. 2011; Pitman et al. 2009). In particular, Pielke et al. (2011) employed both models and observations to demonstrate how land-use changes have impacted surface fluxes at various spatial scales. As a result, the U.S. National Research Council (Jacob et al. 2005) has recommended expanding research into the influence of land-cover processes on climate as a forcing. It has been conjectured that the climate response to land-use and land-cover change could possibly even exceed greenhouse gas contributions, making for very important local, regional, and even global implications (Dirmeyer et al. 2010).

While other studies have investigated the Southeast warming hole by resolving global and regional climate models (Saxena and Yu 1998; Portmann et al. 2009; Rogers 2013), there is considerable uncertainty on the details of the parameters in land-use models, especially at coarse resolution (Pleim and Xiu 2003; McNider et al. 2005). Thus, it is the intent of this paper to investigate this regional anomaly from an observational perspective but within the conceptual framework of variations in the energy budget, specifically as a result of the land-use shift. Long-term temperature and land-cover datasets will be employed to examine the linking trends. Eddy flux tower data will be compiled over the region along with satellite data and a crop model to quantify the different biogeophysical characteristics associated with the major LULC changes. The goal of this paper is to estimate a net

radiative forcing from several perspectives as a result of the LULC change. The analyses will also be supported by skin temperature and albedo observations from satellite-mounted instruments.

2. Biogeophysical land-cover/climate studies

Among the literature, the specified impacts of LULC changes on the local, regional, and global climate vary in strength and sign (Pitman et al. 2009; Findell et al. 2007, 2009). Findell et al. (2009) employed the GFDL Climate Model to investigate relative impacts of land-use change and SST on global and regional temperatures. Results showed that globally, SST is the more important factor, but in regions where significant land-use change has occurred, the LULC signal can be dominant but does not propagate beyond the disturbed region. Depending on the climate, LULC conversions from natural vegetative cover can either increase (tropical) or decrease (temperate) both the temperature and humidity (Mahmood et al. 2014). Regional studies have found that tropical and temperate deforestation can result in warming of 1°–2°C because of an increase in sensible heating resulting from reduced evapotranspiration (ET) rates (Lawrence and Chase 2010; Beltrán-Przekurat et al. 2012; Feddema et al. 2005; among others). Other studies support a cooling trend in the higher latitudes as a result of increased albedo from added agriculture (Bala et al. 2007; Oleson et al. 2004). Beltrán-Przekurat et al. (2012) showed that in temperate South America a simulated conversion from grasslands to agriculture results in cooler temperatures (increased latent heat); however, when converting to agriculture from forested grassland, a warming trend prevailed (decreased latent heat). Trail et al. (2013) suggests that reforestation of cropland in the southeastern United States results in a 0.5-K warming of the surface air due primarily to the albedo effects. The authors arrived at their results by downscaling the Goddard Institute for Space Studies global climate model to the Southeast and performing a sensitivity analysis with respect to albedo and resistance coefficients of different land-use covers. The results were hypothetical and were not compared to any historic data for the region. Similarly, Findell et al. (2007) used the GFDL model to compare 1990 land-cover conditions to natural vegetation conditions globally and regionally. In the Southeast, a change from natural cover (broadleaf and needleleaf forests) to 1990 conditions engendered a decrease in latent energy (LE) at the surface and an increase in sensible heat. Juang et al. (2007) used eddy flux data to show that evergreen forest canopies in the Southeast tend to be significantly cooler than nearby grassland or deforested sites. They showed that although decreased albedos over forested areas do tend toward warming, the changes in ecophysiological and aerodynamic effects are opposite in sign and more than offset the albedo impacts. With respect to cropland in general, irrigation likely adds a cooling effect (Kueppers et al. 2007; Christy et al. 2006), where in theory the maximum temperatures are decreased because of increased latent heating, while to a lesser extent the minimum temperatures have the possibility to increase because of an expanded heat capacity (Misra et al. 2012). As it now stands, studies that include midlatitudes are often mixed in their findings, where both the hydrological and radiative forcings compete.

However, the remotely sensed observations tell a clearer picture. Studies based on satellite observations have consistently shown that southern forests are cooler

than the surrounding deforested areas (Jackson et al. 2008; Wickham et al. 2014, 2012). Wickham et al. (2014) demonstrated that biophysical and surface roughness effects associated with forest canopies tend to offset the albedo warming impacts in U.S. forests south of 36° latitude. It is hypothesized that the year-round latent heat effects and leaf area index associated with evergreen forests in particular, which are more prevalent in the south, account for the anomaly.

Urbanization can also have an effect on the climate, specifically from added aerosols from pollution and increased heat capacity from the urban heat island effect (Karl et al. 1988). Temperature extremes of the twentieth century have been found to be influenced by urbanization (DeGaetano and Allen 2002), due in part to the lack of surface moisture (Li and Bou-Zeid 2013). However, urban growth has not been as significant in the southeastern United States as it has in the Northeast, so urban heat effects would not be expected to be as widespread in the region where in many areas the population has significantly declined.

3. Data and methodology

3.1. Study area

The region of study for this investigation will be the Southeast United States as defined by the regional analysis of McNider et al. (2011, 2014). Figure 3 provides a map of the study area, delineated by National Oceanic and Atmospheric Administration (NOAA) climate divisions, containing the states of Alabama, Georgia, South Carolina, and northern Florida. Though typically included in the southeastern analyses, southern (peninsular) Florida is excluded from this study as the region has experienced anomalous LULC patterns (an increase in agriculture) as compared to the greater area, represents a markedly different climate, and is not contained within the aforementioned warming hole.

3.2. Datasets utilized

3.2.1. LULC

Chen et al. (2006) reconstructed an annual, historical, gridded, land-cover dataset from 1860 to 2003 for the southern United States with a spatial resolution of 8 km. Created to analyze the effect of land-cover change on terrestrial carbon dynamics over the southern United States, the dataset combines several sources, including the global land cover 2000 (GLC2000), the 1992 National Land Cover Dataset (NLCD), the global potential vegetation data, historical cropland county-level data during 1850–1997 from the Census of Agriculture, and the state-level urban area survey data from the USDA Economic Research Service. The Chen et al. (2006) data, hereinafter referred to as the Chen06 dataset, was constructed primarily for forest process studies and did not include a large number of other classes. Therefore, some other land-use datasets that covered all or part of the century were used in conjunction with Chen06.

Historical cropland county-level data dating from 1850 through 1997 (Waisanen and Bliss 2002) were used for further comparison and to extend the Chen06



Figure 3. Study area of the southeastern United States.

classification. In addition, Steyaert and Knox (2008) have also reconstructed a 20-km, historical, biophysical, land-cover dataset of the eastern half of the conterminous United States at 1650, 1850, 1920, and 1992 time intervals. The Steyaert and Knox (2008) dataset combined the county-level census data, potential vegetation, soils data, resource statistics, a Landsat-derived land-cover classification, and published historical information on land cover and land use. The two latter years (1920 and 1992) were utilized in this study and captured the major conversion that occurred midcentury. Other LULC images were also incorporated for the visual purposes of comparison and further validation of the reconstructed datasets. The Multi-Resolution Land Characteristics Consortium's (MRLC; www.mrlc.gov) NLCD is the most widely used LULC data. NLCD consists of 16 land-cover classifications and has been applied consistently across the United States at a spatial resolution of 30 m using Landsat Enhanced Thematic Mapper Plus (ETM+) satellite data. NLCD data exist for the years 1992, 2001, 2006, and 2011; however, only the 1992 image is used here. The enhanced historical land-use and land-cover datasets of the U.S. Geological Survey [Geographic Information Retrieval and Analysis System (GIRAS); Price et al. 2007] provides a composite image of the land use between 1970 and 1985. The USGS dataset's basic sources are NASA high-altitude aerial photographs and USGS National High Altitude Photography (NHAP) program photographs. The data are delineated to actual boundaries with a native resolution of 0.2 to 0.4 km. Further, an image developed from the University of Maryland Department of Geography is used that provides LULC information

Table 1. Eddy covariance tower site locations. The Belle Mina station data began in month 7 and ended in month 10 for one year only.

Station name	State	Location		*n* (days)	Land cover	Months excluded from mean
		Lat (°)	Lon (°)			
Walker Branch	Tennessee	35.9588	−84.2874	1059	Deciduous	
North Carolina Clearcut	North Carolina	35.8115	−76.7115	733	Evergreen	
North Carolina Loblolly Pine	North Carolina	35.8031	−76.6679	1190	Evergreen	
Duke Forest Hardwoods	North Carolina	35.9736	−79.1004	576	Deciduous	
Duke Forest Loblolly Pine	North Carolina	35.9782	−79.0942	770	Evergreen	
Aiken	South Carolina	33.3833	−81.5656	169	Deciduous	4, 6, 7, 8
Austin	Florida	29.7381	−82.2188	449	Evergreen	
Mize	Florida	29.7648	−82.2448	1536	Evergreen	
Donaldson	Florida	29.7547	−82.1633	1598	Evergreen	
Belle Mina Corn Crop	Alabama	34.6886	−86.8879	68	Cropland	7

from AVHRR satellites acquired from 1981 to 1994 (Hansen et al. 2000) at a spatial resolution of 1 km. Combined, this list of LULC datasets provide the best available comprehensive view of LULC change and trends over the southeastern United States for the past century.

3.2.2. Temperature

The National Oceanic and Atmospheric Administration's National Climate Data Center's (NCDC) historical time series of maximum, minimum, and mean monthly temperatures by climate division were used in this investigation (Vose et al. 2014). The data are from the NCDC nCLimDiv database and were derived from a 5-km^2 gridded instance of the Global Historical Climatology Networks daily data. Spatially, average errors are estimated around 1°C over the entire period (Vose et al. 2014).

Surface (skin) temperature data obtained from the Moderate-Resolution Imaging Spectroradiometer (MODIS) were used to further distinguish between temperatures of different LULC. MODIS retrieves two daily land surface temperatures (day and night) at 1-km pixels. Daytime (~1300 local time) images from the summer of 2012 and 2013 are used.

3.2.3. Biogeophysical flux data

The biogeophysical effects of LULC change on temperature include both the change in latent energy and the change in albedo. For this analysis, data from the AmeriFlux network (http://ameriflux.ornl.gov/) of long-term carbon, water, and energy flux measurements were utilized as well as results of a NOAA field campaign in north Alabama. Nine forest eddy flux tower sites (Table 1) were selected for consistency and length of record across the southeastern United States. The vegetation represents evergreen and mixed deciduous canopy covers. Additionally, a cropland (corn) tower from a NOAA field campaign was utilized. The field campaign was conducted at the Tennessee Valley Research and Extension Center

near Bell Mina, Alabama. The study ran from July to October 2014. The AmeriFlux and NOAA data were observed in 30-min intervals and were averaged over each 24-h period. Only days that had a total of 48 observations were used.

Because of the limited amount of available cropland flux data, a crop simulation model [Decision Support System for Agro-technology Transfer (DSSAT); Jones et al. 2003; Hoogenboom et al. 2015] was also employed to estimate the latent energy fluxes from agricultural fields. DSSAT is a framework for biophysical modeling and includes a suite of more than 28 different crop models. It simulates crop growth and yield in response to management, climate, and soil conditions. The DSSAT evaporation algorithms have been validated and proven to be good predictors of evapotranspiration, though they tend to overestimate ET (Sau et al. 2004). Maize (corn), a moderate to high consumer of water, was the surrogate crop modeled to represent cropland energy fluxes. The model was run for 50 years (n = 18 263) and averaged over eight agricultural experiment stations throughout the Southeast. Further, the MODIS Global Evapotranspiration Product (MOD16; Mu et al. 2007, 2011) was used. Representative pixels over the majority agricultural areas were chosen throughout the study area, and data from 2000 to 2014 was used (n = 690).

Different LULCs can affect the albedo and possibly counteract the impact of the change in energy flux. In the current state of affairs, the most common source of albedo data is the MODIS 16-day land surface product (MOD43A3). The MODIS product is a global dataset of spatially complete albedo maps computed for both white sky and black sky at multiple wave lengths. In this case, the full broadband black-sky albedo was used. The black-sky albedo is recommended for use in global change studies by the Global Climate Observing System (GCOS; GCOS 2004). The MODIS albedo maps are composite 16-day images that are updated every 8 days at 500-m spatial resolution.

3.2.4. Incoming solar radiation

The solar radiation data used in this study was the National Land Data Assimilation (NLDAS)-2 surface downward shortwave radiation forcing dataset. The data are formed from bias-corrected GOES satellite solar insolation observations. The GOES Surface and Insolation Products (GSIP) include hourly downward shortwave radiation measurements from the GOES imager over the Northern Hemisphere at a spatial resolution of ⅛°. Here, we assimilate the hourly observations into daily (24 h) values that are then converted to monthly averages over the study area. NLDAS data from the period 2002 to 2009 were utilized in the study.

3.3. Methodology

As mentioned above, the objective of this study was to estimate the change in energy forcing due to the reduction in cropland and coincident increase in forest land over the Southeast. The study period for this analysis covered the years 1920–92. This period is necessary to fully incorporate the USGS LULC dataset. The beginning year coincides with the start of temperature decline, and the range fully encapsulates the overall LULC trends for the region.

The first step in the analysis was to use the various LULC datasets described above to produce one composite land-cover dataset for the study period. The Chen06 forest and the USDA agricultural survey data provided the framework, and the other datasets were used to extend the classifications and fill in missing classes.

Second, the annual, summer, and winter maximum, minimum, and mean temperature data and trends were analyzed and examined against the trends in LULC change for an initial look at the correlation and possible influence and dependence of the two phenomena. Next, samples of MODIS land surface temperatures were examined for the LULC classes that incorporate the majority of the cover change. Finally, eddy flux tower measurements, MODIS ET products, and a crop biophysical model were used to quantify the different biogeophysical characteristics of the changing LULC. A net radiative forcing was then calculated considering all relevant factors.

4. Analysis and results

4.1. LULC classification

Each LULC dataset defines somewhat different classes and were created with specific purposes. In general, the datasets define a range of different LULC by vegetation species, anthropogenic development, and/or natural features to differentiate between biophysical characteristics. To compare the different LULC classes, similar aggregate classes were developed.

In general, to allow for comparison among all LULC datasets, each LULC class represented in the region from all datasets considered were lumped into 11 initial classes as shown in Table 2 below. For the most part, the class aggregation is intuitive. The dataset with the most generalized distinction was used as the common denominator. This allows for datasets like that of Chen06 and USGS with multiple forest classifications to be lumped into three general classes of evergreen, deciduous, and mixed. The urban class is an amalgamation of the impervious area from the Chen06 dataset and the more nuanced classes of the other sets. To better distinguish between biophysical characteristics, agricultural classes were split between cropland, specifically row crops, and pasture land (here categorized as grassland). A common class between three of the five datasets presented here is that of transitional. This LULC class is defined by the USGS as land disturbed because of logging or clearing. In the nineteenth century, it most likely represented land in transition from forest to agriculture or large-scale logging; however, in the twentieth century it would be the opposite, regrowing forest from abandoned cropland and managed timber (Steyaert and Knox 2008).

In Table 2 each LULC dataset was resampled to the county level then area weight averaged over the Southeast. The years 1920, 1950, 1980, and 1992 are presented to give a century-long picture of LULC and showcase each dataset. The AVHRR and GIRAS data represent composite images from the late 1970s through the 1980s.

4.2. LULC change analysis

As is evident from Table 2, the LULC classes that have changed the most in the southeastern United States during the past century are cropland and forest (e.g., see Chen06 and USGS). Looking at the land-cover change fractions at the bottom of

Table 2. Comparison of different LULC datasets for the southeastern United States in faction of land area. See text for description of each dataset.

	LULC class	Evergreen forest	Deciduous forest	Mixed forest	Cropland	Grassland	Urban	Shrubland	Wetland	Transitional	Water	Other
1920	Chen06	0.610	0.070	—	0.206	0.023	0.001	0.000	0.084	—	0.006	0.000
	USDA	—	—	—	0.289	—	—	—	—	—	—	—
	USGS	0.000	0.026	0.456	0.312	0.006	0.048	0.078	0.051	0.000	0.023	—
1950	USDA	—	—	—	0.247	—	—	—	—	—	—	—
	Chen06	0.636	0.074	—	0.175	0.022	0.001	0.000	0.085	—	0.006	0.000
1980	Chen06	0.700	0.088	—	0.087	0.028	0.001	0.000	0.089	—	0.006	0.000
	USDA	—	—	—	0.153	—	—	—	—	—	—	—
	AVHRR	0.187	0.037	0.422	0.089	0.231	0.015	0.000	—	—	0.020	0.000
	GIRAS	0.234	0.061	0.309	0.250	0.001	0.034	0.001	0.083	0.005	0.017	0.005
1992	Chen06	0.723	0.097	—	0.049	0.031	0.003	0.000	0.090	—	0.006	0.000
	USDA	—	—	—	0.126	—	—	—	—	—	—	—
	USGS	0.095	0.026	0.443	0.203	0.006	0.027	0.001	0.123	0.041	0.034	—
	NLCD	0.245	0.176	0.147	0.128	0.078	0.026	0.001	0.127	0.042	0.024	0.006
1920–92 change	Chen06	0.113	0.027	—	−0.157	0.009	0.002	0.000	0.006	—	0.000	—
	USDA	—	—	—	−0.163	—	—	—	—	—	—	—
	USGS	0.095	0.000	−0.013	−0.109	0.000	−0.021	−0.077	0.071	0.041	0.011	—

Table 2, one can see that 95% of all LULC change from 1920 to 1922 is represented by the forest and cropland categories according to the Chen06 dataset (29.4% out of a total change of 31.1%). The USGS dataset, on the other hand, has these two classes composing 52% of the total LULC change (21.7% of 41.7% total). However, the USGS dataset also shows the eastern mixed shrubland decreased by nearly 8%, wetland increased by 7%, and the transitional class increased by 4%, while the Chen06 showed virtually no change in these categories (note that transitional is not present in Chen06). These latter three classes compose another 40% of the total LULC change estimate by the USGS dataset.

In the Chen06 data, the majority of the 15.7% loss in cropland area is replaced by forested land. This is evident as the total of all other LULC change is less than 4% of the overall change. The USGS data do not paint as clear of a picture. However, when the considering the ambiguity of the land-use classes of shrubland and transitional, certain assumptions can be made to make the two datasets more compatible. Assuming that the transitional class represents either clear-cut/logged areas or abandoned farmland transitioning to forests, all of the USGS transition class can be assigned to forest with a high degree of confidence. Next, the USGS forested wetlands class can be assigned as forests, while the herbaceous wetlands are left in the wetlands class. With these changes in the USGS dataset, the forest class increased roughly 15% over the 70-yr period in the Southeast as compared to 14% in the Chen06 data.

The cropland change analysis was done in a similar manner, only using the more reliable USDA county-level crop survey dataset as the baseline. The USGS cropland change was estimated at 10.9%, noticeably lower than both the Chen06 and USDA datasets. The USDA agricultural survey estimates that southeastern cropland decreased 16.3% over the study period, from 28.9% in 1920 to 12.6% in 1992. This supports the idea that the 8% reduction in the USGS shrublands class may very well include overgrown/abandoned cropland in transition to forest. If the USGS cropland data are made to conform to the more reliable USDA survey data, then it can be assumed that the loss in USGS shrublands can actually be assigned to the cropland category, resulting in roughly 16% cropland loss and an associated 3% shrubland loss remaining.

Figure 4 presents the change in forested and cropland land classifications described in the Chen06 and USGS datasets under the assumptions above, while Figure 5 shows a breakdown of LULC change by all categories for both Chen06 and USGS data. Of the change in the forested land, the majority of conversion has been to evergreen stands. The Chen06 dataset shows that of the total 14% growth in forest; temperate needleleaf evergreen forest contributed to nearly 11.3% of that growth. This is consistent with the fact that much of the abandoned farmland was converted to pine plantations in the south. However, when assigning the USGS transitional class to forests, the historic breakdown of evergreen and deciduous forests was followed in order to not unduly bias the results. Figure 5 shows that while the exact percentages of each land-use class are not the same between the datasets, the changes are very similar.

4.3. Temperature trend analysis

The National Climate Data Center's gridded annual minimum, maximum, and mean least squares temperature trends for the United States by climate division for

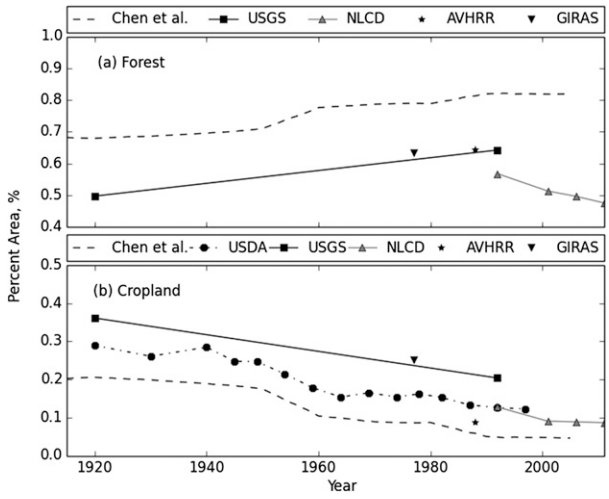


Figure 4. Reconstructed land-cover changes in the southeastern United States from 1920 through 1992 for (a) forest and (b) cropland.

the period 1920 through 1992 are shown in Figure 6. The largest least squares trends are in the southeastern region, generally centered over parts of Alabama and Mississippi. The spatial extent of the negative trends is greater in maximum temperatures. On average, the United States saw an increase of 0.01°C in annual-mean temperatures, while the Southeast (as defined by the study area in Figure 3) declined by a rate of 0.6°C over the same period.

Figure 7 shows the Southeast seasonal trends in minimum and maximum temperatures for the aforementioned time slice, and Table 3 contains the trend slope values and significance. Regime shift analysis (Rodionov 2004) was performed on the data, as is shown by the gray dashed line. The Southeast temperatures show a consistent negative trend among all seasons for both maximum and minimum temperatures. The mean trends for all seasons are statistically significantly nonzero to the 95% percentile. The most negative trends occurred in the winter with minimum temperatures the most negative (−1.46°C). In the summer, maximum temperatures showed the most negative trend (−0.70°C). Annual maximum and minimum temperature trends are nearly equal at 0.60° and 0.59°C, respectively. All tiles in Figure 7 show a significant regime shift to a lower-mean value occurring at a period between 1955 and 1965, with the exception of wintertime minimum temperatures.

4.4. Satellite skin temperature

Next, the difference in temperatures between forested and cropland areas are demonstrated. A look at the observed MODIS skin temperature data shows that forested areas are indeed cooler. Figure 8 shows composite mean MODIS skin temperatures in the Southeast for July 2012 (a significant dry period for most of the region) alongside the MODIS LULC scheme. The visual relationship between land

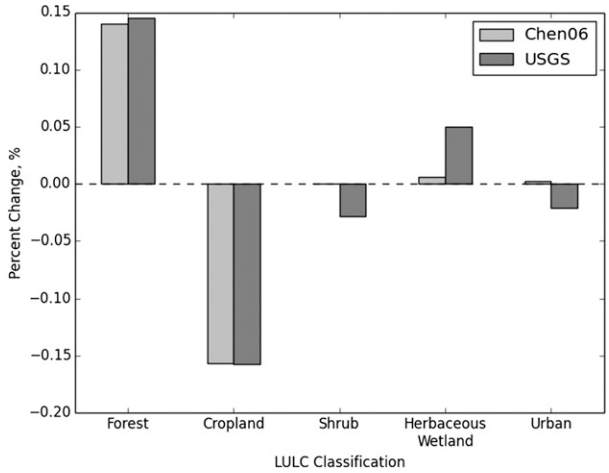


Figure 5. LULC change in the southeastern United States by aggregate classifications from 1920 through 1992.

surface classes and skin temperature is remarkable. The LULC forested classes are shown lumped together in one category together with the major (>95% of the area) LULC classes. It is easily observable that the cropland areas are in general warmer than the adjacent forested areas. Three 30-min latitude bands from a mean January, May, and September composite of 2012 were analyzed, and the spread of the surface temperatures by vegetative LULC classes are shown in Figure 9.

For all months among all latitudes slices, the forested areas on average are observed to have cooler skin temperatures. The mean differences between forest and cropland ranged from 5.50°C (May, 34° slice) to 1.09°C (January, 34° slice). These observations confirm the earlier studies that showed forest canopies cooler, even in winter, than surrounding areas in the southern latitudes (Jackson et al. 2008; Wickham et al. 2012, 2014).

4.5. Analysis of flux data

Figure 10 displays the latent energy (LE) flux data from the 10 Southeast evergreen (Figure 10a) and deciduous (Figure 10b) tower stations. The boxplots display the daily data from all towers; the bold line represents the mean monthly LE and excludes any locations that have less than 10 days of data for a given month as the sample size is not fully representative of the period in question (see Table 1).

The mean of the monthly maximum LE flux towers for evergreen forests was 109.06 W m^{-2}, ranging from 81.52 to 131.14 W m^{-2} with a standard deviation of 18.45 W m^{-2}. The mean monthly minimum LE flux for evergreen forest was 26.81 W m^{-2}, ranging from 18.94 to 33.80 W $m^{-2}$with a standard deviation of 6.59 W m^{-2}.

The mean monthly maximum LE flux for deciduous forest towers was 103.90 W m^{-2}, ranging from 83.04 to 117.01 W m^{-2} with a standard deviation of

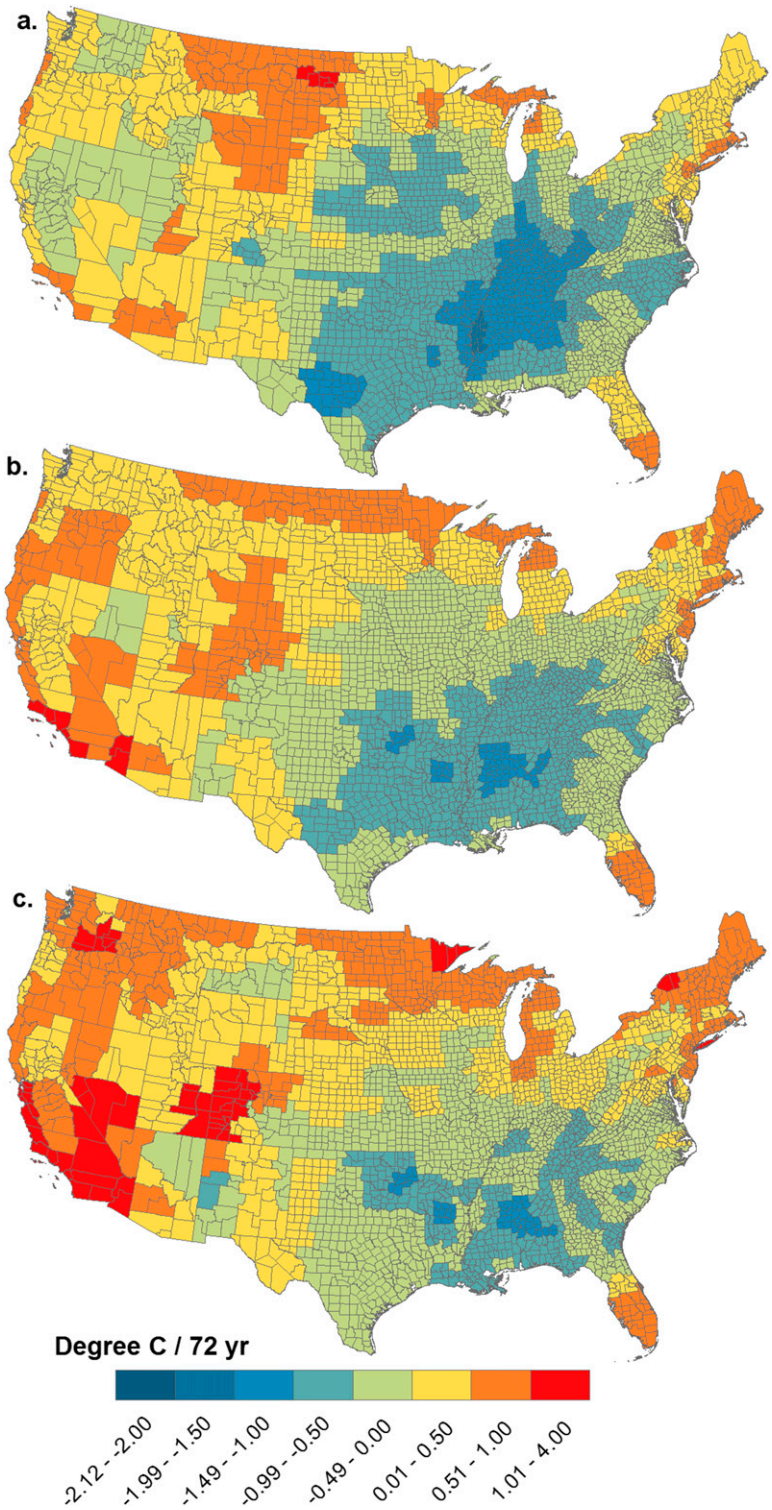


Figure 6. Annual least squares (a) maximum, (b) mean, and (c) minimum temperature trends over the United States by climate division from 1920 to 1992.

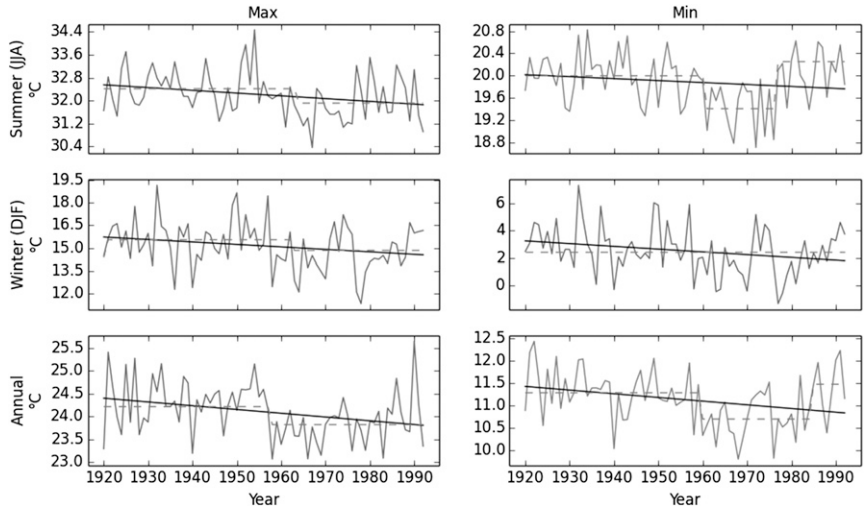


Figure 7. Southeast U.S. seasonal and annual temperature trends (1920–92).

18.26 W m^{-2}. The mean monthly minimum LE flux for deciduous forest was 17.78 W m^{-2}, ranging from 12.89 to 22.85 W m^{-2} with a standard deviation of 4.98 W m^{-2}.

These data are averaged together to get an overall annual distribution of latent energy fluxes for the southeastern United States, represented by the bold lines in Figure 10. Mean values were calculated for each tower; then, the towers were averaged together before the overall annual distribution was calculated to allow towers with more data to be weighted as such. The spatial averaging inevitably smooths out subregional distributions; however, all towers exist within a latitude band of less than 7° and can be assumed to represent similar climates.

Given the lack of observed cropland flux data in the region (data from the 3-month NOAA field campaign over corn), these results needed to be supplemented

Table 3. Regression statistics for temperature trend analysis 1920–92. Bold values indicate trend is significantly nonzero at *p* value = 0.05.

			1895–2014 Trend	1920–92 Trend
Southeast	Winter	Max	+0.64	−1.18
		Min	+0.30	**−1.46**
		Mean	+0.47	**−1.32**
	Summer	Max	−0.44	**−0.70**
		Min	+0.15	−0.25
		Mean	−0.14	**−0.47**
	Annual	Max	+0.04	**−0.60**
		Min	+0.03	**−0.59**
		Mean	+0.04	**−0.59**
United States	Annual	Max	**+0.85**	−0.27
		Min	**+1.04**	+0.31
		Mean	**+0.88**	+0.01

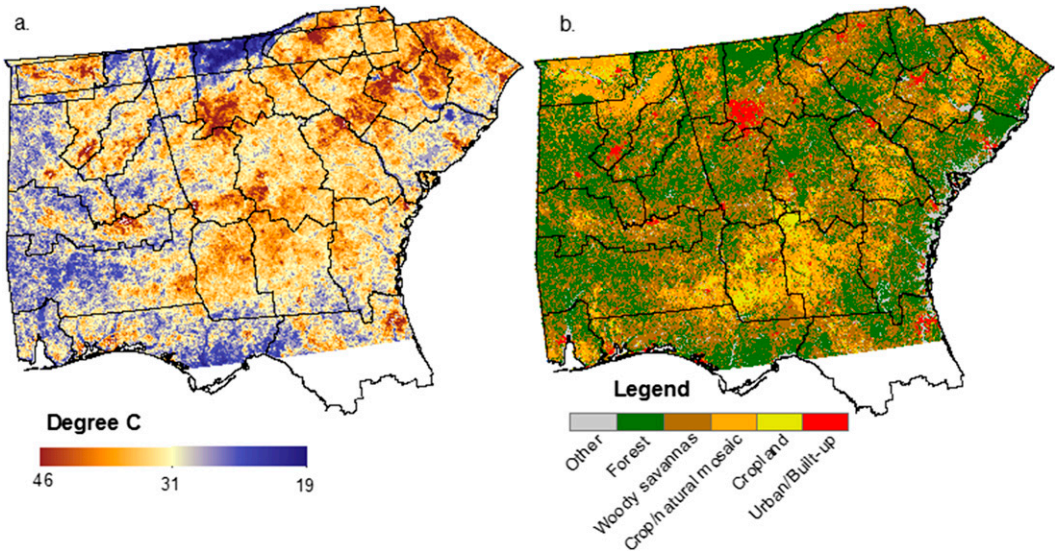


Figure 8. (a) Average July 2012 MODIS skin temperatures and (b) 2012 MODIS land cover.

in order to provide additional data at longer time series and greater spatial coverage. To that end, runs from a biophysical crop growth model DSSAT (Jones et al. 2003; Hoogenboom et al. 2015) and MOD16 (Mu et al. 2011) flux estimates from areas judged to be majority cropland were used to construct a composite seasonal latent energy flux. The estimated seasonal cropland LE is presented in Figure 11, and the mean distribution is represented by the bold line. The mean for the cropland distribution assumes equal monthly weighting for all three datasets.

The estimated mean of the maximum monthly LE fluxes for cropland areas was 81.97 W m^{-2}, ranging from 59.1 to 96.05 W m^{-2} with a standard deviation of 19.98 W m^{-2}. The earliest monthly maximum occurred in May via the DSSAT model, while the MODIS maximums occurred in July. The DSSAT distribution of latent energy fluxes is strongly influenced by planting date, which in these runs was late March. The NOAA Belle Mina corn tower maximum occurred in August, the earliest month for their period of record. The estimated mean of the monthly minimum LE fluxes for croplands was 22.6 W m^{-2}, ranging from 20.91 to 25.53 W m^{-2} with a standard deviation of 2.54 W m^{-2}. The maximum standard deviation within months was 39.43 W m^{-2} and occurred in the DSSAT modeled data for the month of June (6). The average standard deviation within months for all three datasets was 17.17 W m^{-2}.

As seen in Figure 11, there are large variances in the data among the summer months. The cropland maximum LE would be a function of the type of crop planted, planting dates, as well as timing of vital growth stages. Therefore, the occurrence of maximum LE would understandably exhibit a broader range than the evergreen or deciduous forest as shown above. DSSAT shows the crop LE maximums in May and then sharply declines as the corn crop model begins to

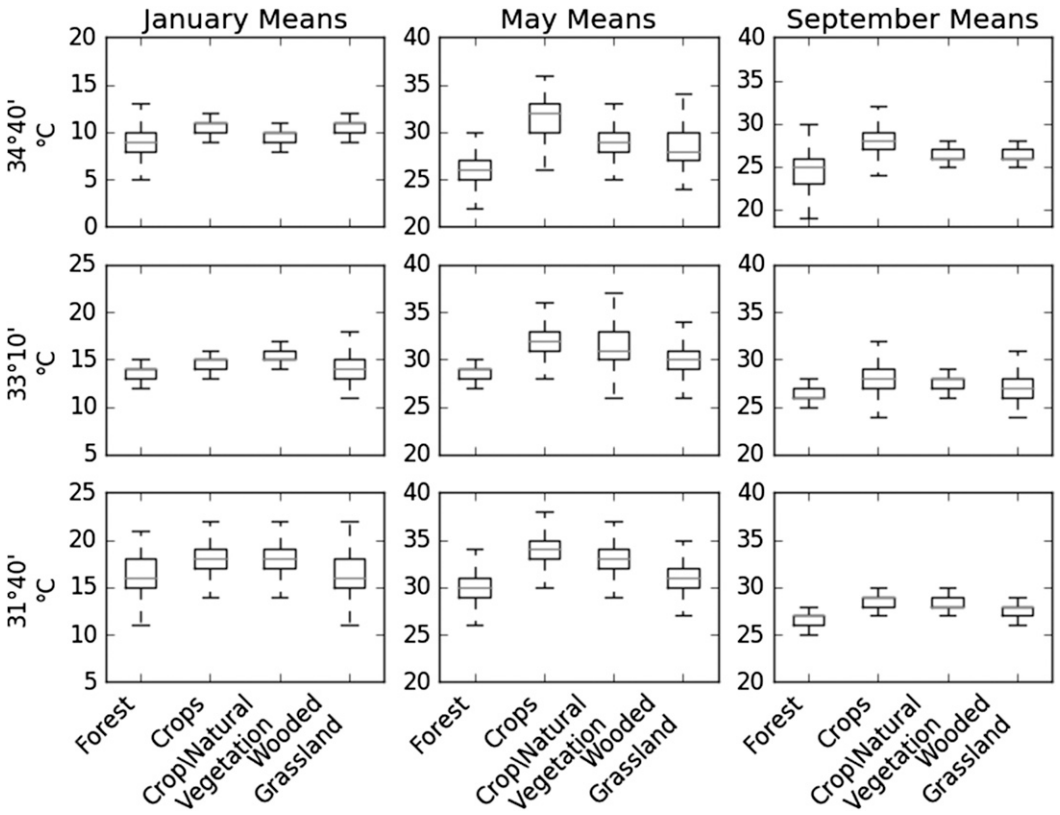


Figure 9. Mean January, May, and September 2012 MODIS skin temperatures by LULC class.

senesce; the Belle Mina tower data corroborates this pattern. Once corn reaches its physiological maturity, water is no longer needed by the crop, and as such ET is diminished significantly. The LE from the MODIS data remains consistently larger through August. The maximum standard deviation among monthly means is 23.82 W m^{-1}, and the overall seasonal mean is represented by the bold line in Figure 11.

The annual LE fluxes for evergreen forest, deciduous forest, and cropland as defined above are 66.7, 54.2, and 47.62 W m^{-2}, respectively. Figure 12 presents the mean monthly latent energies (along with standard errors) for evergreen forest, deciduous forest, and croplands. It is not surprising that, in general, evergreen and deciduous latent fluxes are similar during summer months, while evergreen stands tend to transpire more on average during winter months, as they retain their foliage. Cropland ET exceeds that of deciduous forest ET until the emergence of vegetation concludes in May and then remains less than both forest types for the remainder of the year.

4.6. Albedo data for the southeastern United States

The second major component of the energy budget that is impacted by land-cover change is the albedo. It is generally recognized that in order to gain an

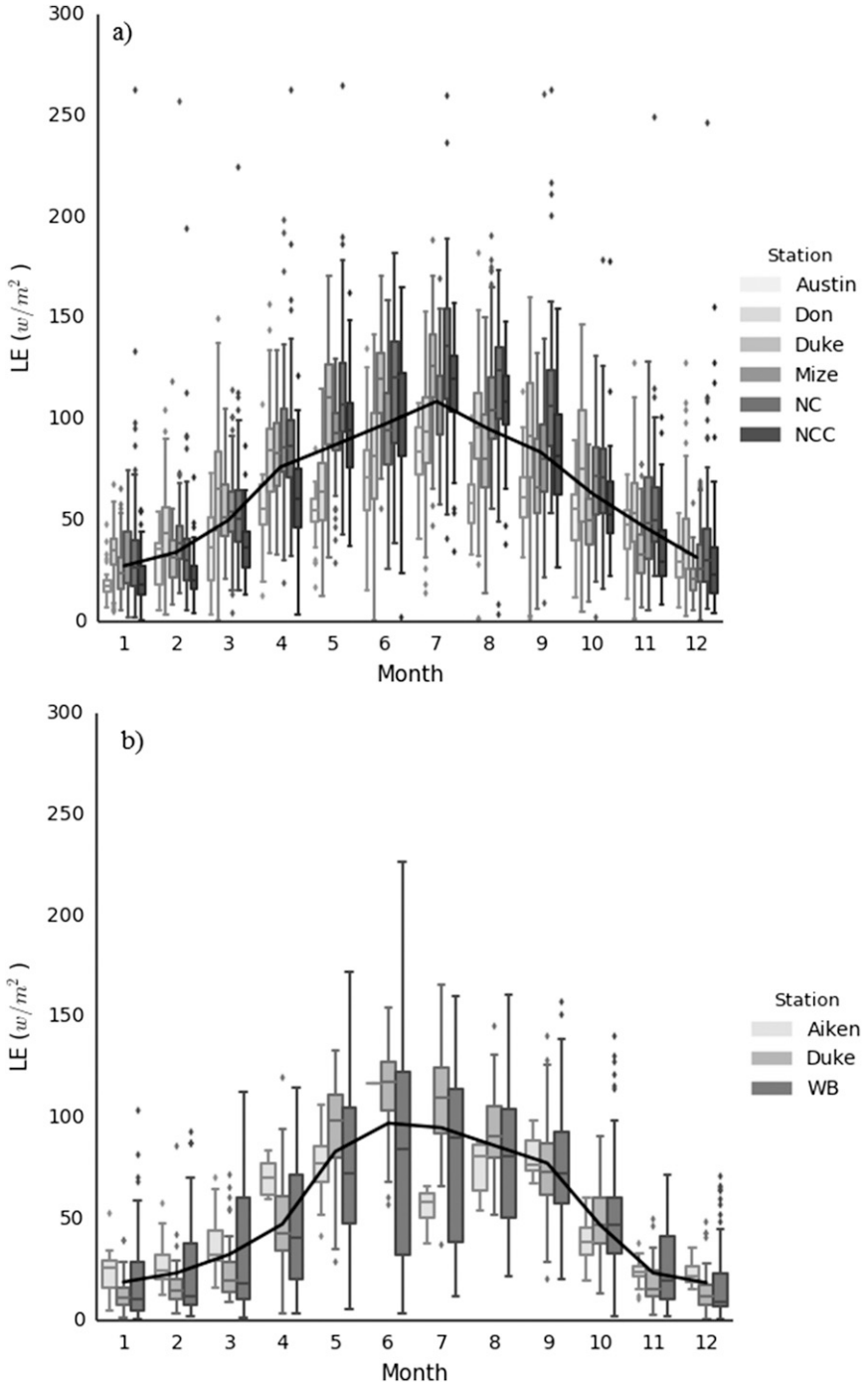


Figure 10. Latent energy flux for (a) evergreen and (b) deciduous forest land covers from selected eddy covariance towers in the Southeast. Boxplot shows the spread among the daily observations, and the solid dark line represents the overall mean annual distribution. Values are determined to be "outliers" when ±1.5 times the interquartile range.

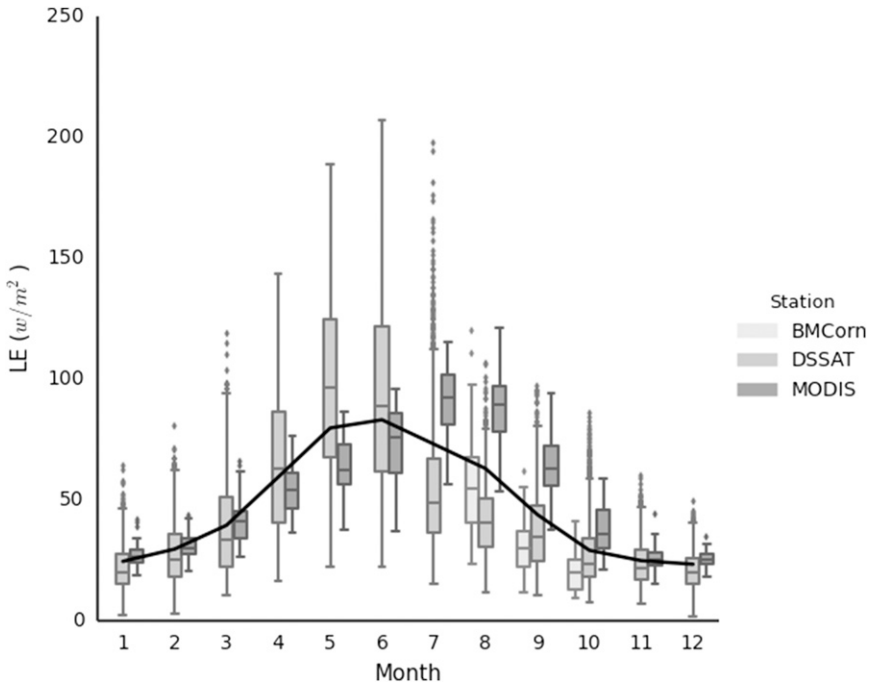


Figure 11. Latent energy fluxes from the Belle Mina, Alabama, cropland tower, the DSSAT crop model (n = 18 236), and representative MODIS cropland pixels (n = 690) for the southeastern United States. The boxplot shows the spread of the daily observations and modeled values, and the dark solid line represents the overall mean annual distribution.

accurate picture of land surface albedo over a large spatial domain, satellite-mounted instruments are necessary. In this study, the MODIS land-cover product was used to determine the land-cover class of each pixel within the albedo coverage described in section 3.2.3 above. Albedo values for pixels with the same land cover were averaged monthly to determine the albedo to be assigned to that land-cover class. The monthly average albedos for each land-cover class are shown in Figure 13.

4.7. Energy budget analysis

Using the datasets that have been accumulated in this study, it is possible to make an estimate of a net change in energy forcings due to latent energy and the effects of albedo changes associated with the land-cover change in the southeastern United States over the study period. The major LULC change that occurred over the past century was from agriculture and cropland to forest, primarily evergreen plantations. A conservative estimate of 15% of cropland went into forest-type land cover. Following the current breakdown of forest species discussed in section 3.2 above, the LULC change was partitioned into categories: cropland to evergreen (12%) and cropland to deciduous (3%). The net differences in latent energy were

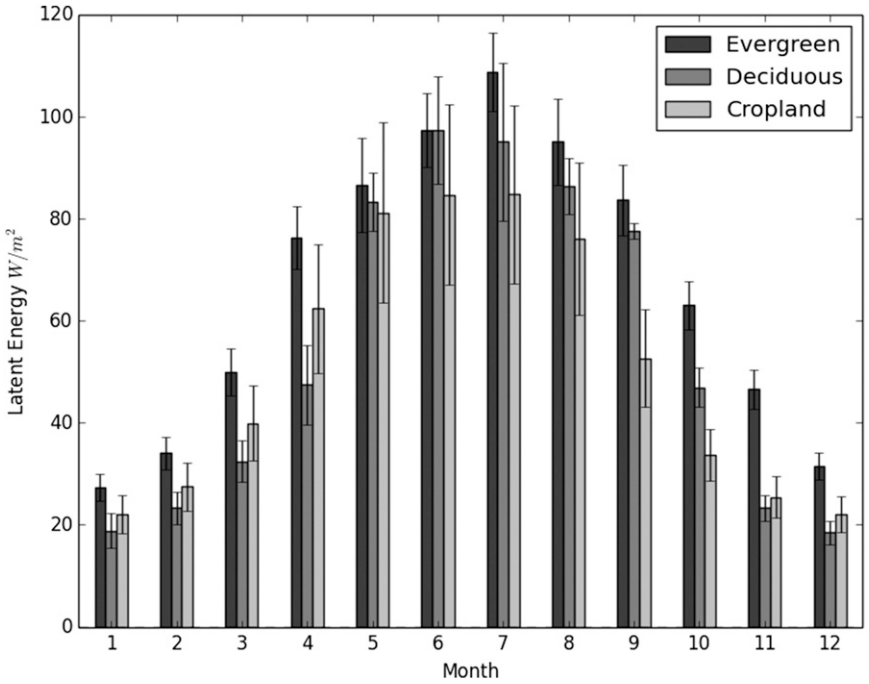


Figure 12. Summary of the mean, monthly latent energy fluxes for forest and cropland LULC classifications. Error bars represent the standard error of the mean.

calculated via the mean annual distributions, applied to the LULC change, and resulted in a mean annual forcing of $-2.5\,\mathrm{W\,m^{-2}}$ due to the increased LE. This equates to a monthly average difference in ET between forests and cropland of about $2.63\,\mathrm{mm\,month^{-1}}$.

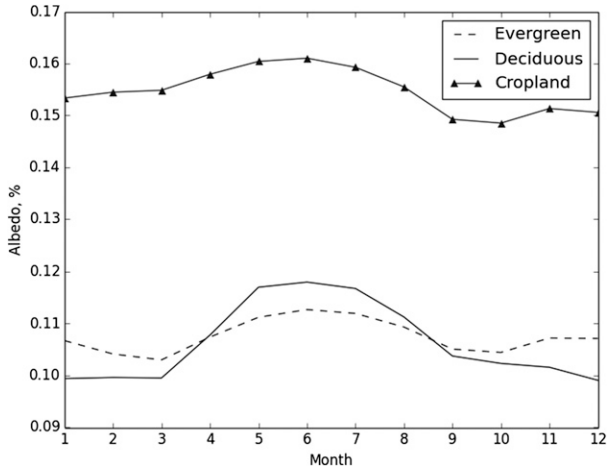


Figure 13. MODIS monthly average (2002–09) black-sky albedos by LULC class.

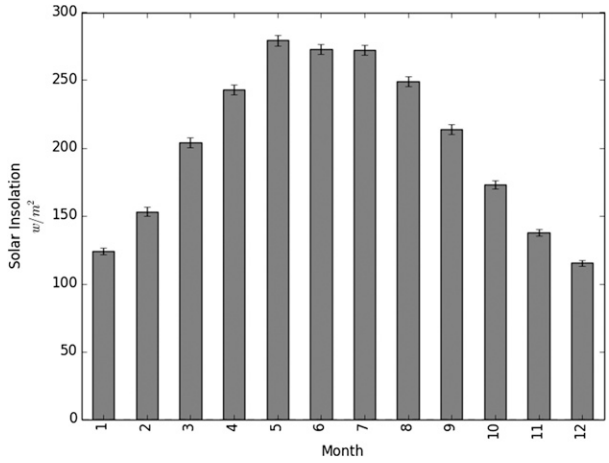


Figure 14. Monthly average of NLDAS incoming radiation: 2002–09. Error bars represent standard errors of the mean.

Next, the annual distribution of albedo was applied to the monthly average incoming shortwave radiation in the region to arrive at the change in energy partitioned because of change in albedo. The monthly average NLDAS incoming shortwave radiation data described in section 3.2.4 above is shown in Figure 14. Though the incoming shortwave is averaged over a large area, the monthly values' maximum standard deviations spatially across the region are on average less than 10%. The overall mean standard deviation for the shortwave data is 14.44 W m^{-2}. The analysis assumes a consistent, monthly, incoming radiation over the study period based on the 2002–09 NLDAS data. This is done to exclude other extraneous effects such as solar dimming, cycles, and so on, in order to isolate the effects of land-use change only. By applying the incoming shortwave to the annual distribution of albedo (Figure 13) and the associated LULC change percentages, the resultant mean annual change in reflected shortwave solar radiation is determined to be $+1.44$ W m^{-2}.

Figure 15 shows the annual distribution of the combined net forcings due to the estimated LULC change under the assumption that all of the reflected energy from the changes in albedo would go into sensible heat. The southeastern United States resides in a humid, subtropical climate, and in this energy-limited, water-rich environment, the latent energy is mostly governed by the available water. Under this assumption, the results show that the change in sensible (as a result of albedo) and latent energies are in direct competition with each other. In the spring and early summer months, the croplands are in peak production, and the latent energy associated with their ET is comparable to that of the forested areas, so the positive change in radiation due to albedo dominates the signal, thus creating a positive forcing. Not surprisingly though, the late summer and fall months are the largest contributors to an overall negative sign of the forcing as this is the time when major crops have matured (or been harvested), thus reducing their transpiration rate as compared to the forest. At this point, bare soil evaporation would be the major source of latent energy for these areas. On the other hand, forests (particularly

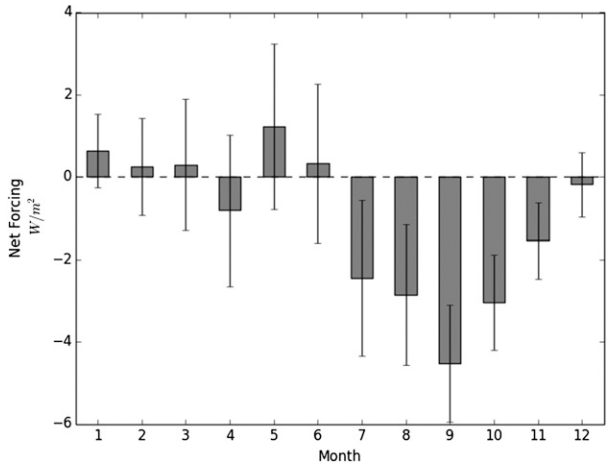


Figure 15. Annual distribution of the net radiative forcing considering latent heat and albedo affects.

evergreens) maintain their foliage and, with their deep roots, are able to continue to transpire as long as atmospheric conditions are favorable. Overall, the mean annual net radiative forcing as a result of the LULC change from cropland to forests is estimated to be $-1.06\,\mathrm{W\,m^{-2}}$. This figure might be conservative (i.e., too high) because of the assumption that all the changes in reflected energy would go to sensible heat. If some small portion of this energy added to the latent heat component, then the combined forcing estimate would be even lower (more negative).

5. Discussion

The largest errors exist in the latent flux data and the albedo. The standard error of the monthly means was used to describe the error of latent fluxes (Figure 12), while values taken from the literature were used for the albedo. The overall mean standard error for the latent flux component was $6.19\,\mathrm{W\,m^{-2}}$. The maximum standard error of the mean for the latent flux data, $17.83\,\mathrm{W\,m^{-2}}$, resulted from the cropland fluxes that incorporated multiple sources. The evergreen flux data mean errors were considerably lower than that of the cropland and deciduous data: $4.21\,\mathrm{W\,m^{-2}}$ as compared to 7.29 and $7.03\,\mathrm{W\,m^{-2}}$, respectively. The standard errors among the monthly MODIS albedo data were minimal; however, the MODIS albedo algorithm has been tested against ground-based data (Wang et al. 2014; Cescatti et al. 2012), and average errors were found to be on the order of 0.02 for forested areas and 0.03 for cropland and mixed-use agricultural areas.

Errors in the deciduous data are most likely the resultant of a sample size as only three towers were available. However, the errors in the cropland data are more inherent. Crops, being more sensitive to the yearly variations in weather, are subject to short-term droughts, different phenological responses, and different cultural practices (fertilizer applications, tillage, etc.). Additionally, the MODIS 1-km (ET) and 5000-m (albedo) pixel footprints often incorporate a more diverse landscape than cropland alone, usually consisting of a mosaic of crops, trees, and grassland.

The full spread of errors among the mean net forcings is shown in Figure 15. The error bars represent the maximum deviation based on all propagated errors. The monthly mean forcing of -1.06 resides in a confidence interval of $\pm 3.35\ \mathrm{W\ m^{-2}}$.

A simple but typical model for the short-term rate of change of surface temperature can be given by (Blackadar 1979; Noilhan and Planton 1989; McNider et al. 1994; Pleim and Xiu 2003)

$$\frac{\partial T_G}{\partial t} = \frac{1}{c_g}[R_L + (1 - \alpha_S)R_S - \varepsilon\sigma T_S^4 - H - E - G].$$

Here, T_G is the ground/canopy temperature, c_g is the heat capacity/thermal resistance of the surface, R_L is the longwave downward radiation, R_S is the incoming solar radiation, α_S is the surface albedo, T_S is the surface or radiating temperature, ε is the surface emissivity, σ is the Stefan–Boltzmann constant, H is the sensible heat flux, E is the evaporative heat flux, and G is the ground heat flux.

In climate or regional weather models such equations have been used to model LULC impacts if the fundamental parameters associated with the land-use class (e.g., c_g or surface moisture) can be specified. However, as found by differences in the LULC model results discussed above, and simply because of the difficulty in defining a priori parameters (McNider et al. 2005), there is uncertainty in such applications. However, the equation can be used as a framework to discuss differences in energies between forests and croplands. Above, we have explored the effects of both the latent heat E and albedo α. Another potentially significant component when discussing the energy budget over forest and cropland is the thermal resistance or heat capacity c_g of the two land-use types. As noted by McNider et al. (2005) and Pleim and Xiu (2003), the specification of the thermal resistance of a canopy is difficult since many ill-observed physical processes govern the parameter-leading c_g values to vary by several orders of magnitude across different land-use schemes. McNider et al. (2005) argued that it is in fact a model heuristic for practical mixed grids found in the real world.

However, it is almost certain that the heat capacity of mature forests exceed that of cropland. Cropland heat capacity also is a function of season with higher values during mature growth periods (due to water content), distribution of energy interception, and mixing processes within the canopy.

Using a technique to back calculate a heat capacity through use of Equation (1) and use of geostationary skin tendencies, McNider et al. (2005) found a difference of a factor of 3–5 in c_g between forest areas and agricultural areas in the Mississippi delta region. Thus, some of the differences in the MODIS skin temperature data shown in Figure 9 are due to the greater thermal resistance of forests to insolation and not just changes in latent heat flux. While the factor of 3–5 in c_g might appear based on linear scaling to be the biggest difference in Equation (1), as shown by Mackaro et al. (2012), in such a nonlinear system, linear parameter relationships do not hold.

Additional energetic impacts of the LULC change, such as longwave changes due to E, changes in shortwave fluxes due to cloud cover, and ground flux contributions beyond those tied to the heat capacity, were not considered. Though, as discussed by Yang et al. (1999), soil heat flux is much less in vegetated land covers due to reduction in the incoming radiation by the canopy. In those cases, the heat

capacity of the vegetation and soil are sometimes combined, so the conclusions as to the heat capacity effects discussed in the previous paragraphs would also include the ground flux. A complete estimation of the impact of LULC change from agriculture to forests will require full modeling with a model that can physically reproduce the MODIS image skin temperature image in Figure 9. However, the analysis given here indicates a negative forcing due to increased evaporation. With the inclusion of heat capacity changes, the total results will likely exceed the net $-1.06\,\mathrm{W\,m^{-2}}$ derived above.

6. Conclusions

The IPCC AR5 (2013) estimates that the global land-use changes have increased the surface albedo, leading to a radiative forcing of $0.15 \pm 0.10\,\mathrm{W\,m^{-2}}$. The spread of the data demonstrates that there are still uncertainties in both the fraction of land-cover change as well as albedos, though the AR5 states robust confidence in the sign of the albedo forcing. However, because of other competing consequences, there is little confidence in the sign of the overall net change in temperature due to land-cover change.

This study can be interpreted as support for both of these statements. The confidence in the sign of the global albedo forcing is derived from recent studies showing a net increase in agricultural development of land and an overall decrease in forest cover. The southeastern U.S. LULC trend is the opposite, with cropland declining precipitously over the past century and replaced by forest cover. As such, a positive albedo forcing is observed; however, when the effects of latent energy fluxes are considered, the overall forcing switches to a negative.

Many studies of the southeastern U.S. warming hole have been conducted over the past few years. However, the majority of these studies have relied upon downscaled climate models with sensitivity analysis of specific parameters within the models related to land cover. As a result, their conclusions are more of a hypothetical nature. Alternatively, several authors have used satellite data to demonstrate that forest temperatures are cooler than nearby cropland in the southern latitudes. However, these authors have made no conclusions as to the causal mechanisms of these observations.

In this study, a first attempt at an actual energy budget analysis of the warming hole problem was conducted. The albedo and latent energy terms of the equation were specifically addressed for the dominant land-use change of agriculture to forested land, in particular evergreen. To the extent possible, in situ flux data and observations from satellite-mounted instruments were used to conduct the experiment. It was found that for the southeastern U.S. region, the albedo and latent heat terms are of opposite sign, but, overall, the increase in latent energy associated with the higher transpiration of the evergreen forests compared to cropland more than offsets the positive albedo effect leading to an overall negative forcing. The energy forcing associated with the land-cover change from cropland to evergreen forest was conservatively estimated to be $-1.06\,\mathrm{W\,m^{-2}}$ with a confidence interval of $\pm 3.35\,\mathrm{W\,m^{-2}}$. This, in conjunction with other studies in the literature, provides more confidence in the sign being negative than positive.

Referring to the IPCC report, the overall land-use change impact of $-1.06\,\mathrm{W\,m^{-2}}$ estimated in this study is larger than any other forcing other than CO_2 itself

($+1.68\,\mathrm{W\,m^{-2}}$). Based on this result, it is easy to see how this negative forcing combined with the other components already identified (aerosols, atmospheric particulates, overall dimming, etc.) result in a cooling effect over the Southeast during the majority of the twentieth century.

Acknowledgments. This research was supported under the joint NSF/USDA Project "F/USDA/NIFA Type 2—Collaborative Research—Migration of Agricultural Production Back to the Southeast." Dr. Hanqin Tian and his research team at Auburn University provided the essential forest land-cover dataset and generously aided in its interpretation. Dr. Mohammad Al-Hamdan provided the NLDAS solar radiation data. We gratefully acknowledge their assistance with this work. Additionally, the comments and suggestions from two anonymous reviewers greatly improved the manuscript.

References

Bala, G., K. Caldeira, M. Wickett, T. J. Phillips, D. B. Lobell, C. Delire, and A. Mirin, 2007: Combined climate and carbon-cycle effects of large-scale deforestation. *Proc. Natl. Acad. Sci. USA*, **104**, 6550–6555, doi:10.1073/pnas.0608998104.

Baldocchi, D., and S. Ma, 2013: How will land use affect air temperature in the surface boundary layer? Lessons learned from a comparative study on the energy balance of an oak savanna and annual grassland in California, USA. *Tellus*, **65B**, 19994, doi:10.3402/tellusb.v65i0.19994.

Beltrán-Przekurat, A., R. A. Pielke Sr., J. L. Eastman, and M. B. Coughenour, 2012: Modelling the effects of land-use/land-cover changes on the near-surface atmosphere in southern South America. *Int. J. Climatol.*, **32**, 1206–1225, doi:10.1002/joc.2346.

Blackadar, A. K., 1979: High resolution models of the planetary boundary layer. *Adv. Environ. Sci. Eng.*, **1**, 50–85.

Boisier, J. P., N. de Noblet-Ducoudré, and P. Ciais, 2014: Historical land-use-induced evapotranspiration changes estimated from present-day observations and reconstructed land-cover maps. *Hydrol. Earth Syst. Sci.*, **18**, 3571–3590, doi:10.5194/hess-18-3571-2014.

Bronaugh, W., 2012: North American forests in the Age of Man. *American Forests Magazine*, Summer 2012, accessed 15 June 2015. [Available online at https://www.americanforests.org/magazine/article/north-american-forests-in-the-age-of-man/.]

Cescatti, A., and Coauthors, 2012: Intercomparison of MODIS albedo retrievals and in situ measurements across the global FLUXNET network. *Remote Sens. Environ.*, **121**, 323–334, doi:10.1016/j.rse.2012.02.019.

Chen, H., H. Tian, M. Liu, J. Melillo, S. Pan, and C. Zhang, 2006: Effect of land-cover change on terrestrial carbon dynamics in the southern United States. *J. Environ. Qual.*, **35**, 1533–1547, doi:10.2134/jeq2005.0198.

Christy, J. R., W. B. Norris, K. Redmond, and K. P. Gallo, 2006: Methodology and results of calculating central California surface temperature trends: Evidence of human-induced climate change? *J. Climate*, **19**, 548–563, doi:10.1175/JCLI3627.1.

Crowley, T. J., 2000: Causes of climate change over the past 1000 years. *Science*, **289**, 270–277, doi:10.1126/science.289.5477.270.

DeGaetano, A. T., and R. J. Allen, 2002: Trends in twentieth-century temperature extremes across the United States. *J. Climate*, **15**, 3188–3205, doi:10.1175/1520-0442(2002)015<3188:TITCTE>2.0.CO;2.

de Noblet-Ducoudré, N., and Coauthors, 2012: Determining robust impacts of land-use-induced land cover changes on surface climate over north America and Eurasia: Results from the first set of LUCID experiments. *J. Climate*, **25**, 3261–3281, doi:10.1175/JCLI-D-11-00338.1.

Dirmeyer, P. A., D. Niyogi, N. de Noblet-Ducoudré, R. E. Dickinson, and P. K. Snyder, 2010: Impacts of land use change on climate. *Int. J. Climatol.*, **30**, 1905–1907, doi:10.1002/joc.2157.

Dobrowski, S. Z., J. Abatzoglou, A. K. Swanson, J. A. Greenberg, A. R. Mynsberge, Z. A. Holden, and M. K. Schwartz, 2013: The climate velocity of the contiguous United States during the 20th century. *Global Change Biol.*, **19**, 241–251, doi:10.1111/gcb.12026.

Fall, S., D. Niyogi, A. Gluhovsky, R. A. Pielke, E. Kalnay, and G. Rochon, 2010: Impacts of land use land cover on temperature trends over the continental United States: Assessment using the North American Regional Reanalysis. *Int. J. Climatol.*, **30**, 1980–1993, doi:10.1002/joc.1996.

Feddema, J. J., K. W. Oleson, G. B. Bonan, L. O. Mearns, L. E. Buja, G. A. Meehl, and W. M. Washington, 2005: The importance of land-cover change in simulating future climates. *Science*, **310**, 1674–1678, doi:10.1126/science.1118160.

Findell, K. L., E. Shevliakova, P. C. D. Milly, and R. J. Stouffer, 2007: Modeled impact of anthropogenic land cover change on climate. *J. Climate*, **20**, 3621–3634, doi:10.1175/JCLI4185.1.

——, A. J. Pitman, M. H. England, and P. J. Pegion, 2009: Regional and global impacts of land cover change and sea surface temperature anomalies. *J. Climate*, **22**, 3248–3269, doi:10.1175/2008JCLI2580.1.

GCOS, 2004: Summary report of the eighth session of the GCOS/GTOS terrestrial observation panel for climate. GCOS Rep. WMO/TD 1238, 23 pp. [Available online at http://www.wmo.int/pages/prog/gcos/Publications/gcos-93.pdf.]

Hansen, M., R. DeFries, J. Townshend, and R. Sohlberg, 2000: Global land cover classification at 1 km spatial resolution using a classification tree approach. *Int. J. Remote Sens.*, **21**, 1331–1364, doi:10.1080/014311600210209.

Hartmann, D. L., and Coauthors, 2013: Observations: Atmosphere and surface. *Climate Change 2013: The Physical Science Basis*, T. F. Stocker et al., Eds., Cambridge University Press, 159–254.

Hoogenboom, G., and Coauthors, 2015: Decision Support System for Agrotechnology Transfer (DSSAT) version 4.6. Accessed July 2014. [Available online at www.dssat.net.]

Jackson, R. B., and Coauthors, 2008: Protecting climate with forests. *Environ. Res. Lett.*, **3**, 044006, doi:10.1088/1748-9326/3/4/044006.

Jacob, D., R. Avissar, G. Bond, and S. Gaffin, 2005: *Radiative Forcing of Climate Change: Expanding the Concept and Addressing Uncertainties*. National Research Council of the National Academies Press, 224 pp.

Jones, J., and Coauthors, 2003: The DSSAT cropping system model. *Eur. J. Agron.*, **18**, 235–265, doi:10.1016/S1161-0301(02)00107-7.

Juang, J.-Y., G. Katul, M. Siqueira, P. Stoy, and K. Novick, 2007: Separating the effects of albedo from eco-physiological changes on surface temperature along a successional chronosequence in the southeastern United States. *Geophys. Res. Lett.*, **34**, L21408, doi:10.1029/2007GL031296.

Kalnay, E., and M. Cai, 2003: Impact of urbanization and land-use change on climate. *Nature*, **423**, 528–531.

Karl, T. R., H. F. Diaz, and G. Kukla, 1988: Urbanization: Its detection and effect in the United States climate record. *J. Climate*, **1**, 1099–1123, doi:10.1175/1520-0442(1988)001<1099:UIDAEI>2.0.CO;2.

Knappenberger, P. C., P. J. Michaels, and R. E. Davis, 2001: Nature of observed temperature changes across the United States during the 20th century. *Climate Res.*, **17**, 45–53, doi:10.3354/cr017045.

Kueppers, L. M., M. A. Snyder, and L. C. Sloan, 2007: Irrigation cooling effect: Regional climate forcing by land-use change. *Geophys. Res. Lett.*, **34**, L03703, doi:10.1029/2006GL028679.

Kunkel, K. E., X.-Z. Liang, J. Zhu, and Y. Lin, 2006: Can CGCMs simulate the twentieth-century "warming hole" in the central United States? *J. Climate*, **19**, 4137–4153, doi:10.1175/JCLI3848.1.

Lawrence, P. J., and T. N. Chase, 2010: Investigating the climate impacts of global land cover change in the community climate system model. *Int. J. Climatol.*, **30**, 2066–2087, doi:10.1002/joc.2061.

——, and Coauthors, 2012: Simulating the biogeochemical and biogeophysical impacts of transient land cover change and wood harvest in the Community Climate System Model (CCSM4) from 1850 to 2100. *J. Climate*, **25**, 3071–3095, doi:10.1175/JCLI-D-11-00256.1.

Leibensperger, E. M., and Coauthors, 2012: Climatic effects of 1950–2050 changes in US anthropogenic aerosols—Part 2: Climate response. *Atmos. Chem. Phys.*, **12**, 3349–3362, doi:10.5194/acp-12-3349-2012.

Li, D., and E. Bou-Zeid, 2013: Synergistic interactions between urban heat islands and heat waves: The impact in cities is larger than the sum of its parts. *J. Appl. Meteor. Climatol.*, **52**, 2051–2064, doi:10.1175/JAMC-D-13-02.1.

Mackaro, S. M., R. T. McNider, and A. P. Biazar, 2012: Some physical and computational issues in land surface data assimilation of satellite skin temperatures. *Pure Appl. Geophys.*, **169**, 401–414, doi:10.1007/s00024-011-0377-0.

Mahmood, R., and Coauthors, 2010: Impacts of land use/land cover change on climate and future research priorities. *Bull. Amer. Meteor. Soc.*, **91**, 37–46, doi:10.1175/2009BAMS2769.1.

——, and Coauthors, 2014: Land cover changes and their biogeophysical effects on climate. *Int. J. Climatol.*, **34**, 929–953, doi:10.1002/joc.3736.

McNider, R. T., A. J. Song, D. M. Casey, P. J. Wetzel, W. L. Crosson, and R. M. Rabin, 1994: Toward a dynamic-thermodynamic assimilation of satellite surface temperature in numerical atmospheric models. *Mon. Wea. Rev.*, **122**, 2784–2803, doi:10.1175/1520-0493(1994)122<2784:TADTAO>2.0.CO;2.

——, W. M. Lapenta, A. P. Biazar, G. J. Jedlovec, R. J. Suggs, and J. Pleim, 2005: Retrieval of model grid-scale heat capacity using geostationary satellite products. Part I: First case-study application. *J. Appl. Meteor. Climatol.*, **44**, 1346–1360, doi:10.1175/JAM2270.1.

——, J. R. Christy, D. Moss, K. Doty, C. Handyside, A. Limaye, A. Garcia y Garcia, and G. Hoogenboom, 2011: A real-time gridded crop model for assessing spatial drought stress on crops in the southeastern United States. *J. Appl. Meteor. Climatol.*, **50**, 1459–1475, doi:10.1175/2011JAMC2476.1.

——, and Coauthors, 2014: An integrated crop and hydrologic modeling system to estimate hydrologic impacts of crop irrigation demands. *Environ. Modell. Software*, **72**, 341–355, doi:10.1016/j.envsoft.2014.10.009.

Meehl, G. A., W. M. Washington, C. M. Ammann, J. M. Arblaster, T. M. L. Wigley, and C. Tebaldi, 2004: Combinations of natural and anthropogenic forcings in twentieth-century climate. *J. Climate*, **17**, 3721–3727, doi:10.1175/1520-0442(2004)017<3721:CONAAF>2.0.CO;2.

——, and Coauthors, 2012: Climate system response to external forcings and climate change projections in CCSM4. *J. Climate*, **25**, 3661–3683, doi:10.1175/JCLI-D-11-00240.1.

——, A. Hu, J. M. Arblaster, J. Fasullo, and K. E. Trenberth, 2013: Externally forced and internally generated decadal climate variability associated with the interdecadal Pacific oscillation. *J. Climate*, **26**, 7298–7310, doi:10.1175/JCLI-D-12-00548.1.

Misra, V., J.-P. Michael, R. Boyles, E. P. Chassignet, M. Griffin, and J. J. O'Brien, 2012: Reconciling the spatial distribution of the surface temperature trends in the southeastern United States. *J. Climate*, **25**, 3610–3618, doi:10.1175/JCLI-D-11-00170.1.

Mu, Q., F. A. Heinsch, M. Zhao, and S. W. Running, 2007: Development of a global evapotranspiration algorithm based on MODIS and global meteorology data. *Remote Sens. Environ.*, **111**, 519–536, doi:10.1016/j.rse.2007.04.015.

——, M. Zhao, and S. W. Running, 2011: Improvements to a MODIS global terrestrial evapotranspiration algorithm. *Remote Sens. Environ.*, **115**, 1781–1800, doi:10.1016/j.rse.2011.02.019.

Napton, D. E., R. F. Auch, R. Headley, and J. L. Taylor, 2009: Land changes and their driving forces in the southeastern United States. *Reg. Environ. Change*, **10**, 37–53, doi:10.1007/s10113-009-0084-x.

Noilhan, J., and S. Planton, 1989: A simple parameterization of land surface processes for meteorological models. *Mon. Wea. Rev.*, **117**, 536–549, doi:10.1175/1520-0493(1989)117<0536:ASPOLS>2.0.CO;2.

Oleson, K. W., G. B. Bonan, S. Levis, and M. Vertenstein, 2004: Effects of land use change on North American climate: Impact of surface datasets and model biogeophysics. *Climate Dyn.*, **23**, 117–132, doi:10.1007/s00382-004-0426-9.

Pan, Z., R. W. Arritt, E. S. Takle, W. J. Gutowski Jr., C. J. Anderson, and M. Segal, 2004: Altered hydrologic feedback in a warming climate introduces a "warming hole." *Geophys. Res. Lett.*, **31**, L17109, doi:10.1029/2004GL020528.

Pielke, R. A., G. Marland, R. A. Betts, T. N. Chase, J. L. Eastman, J. O. Niles, D. D. S. Niyogi, and S. W. Running, 2002: The influence of land-use change and landscape dynamics on the climate system: Relevance to climate-change policy beyond the radiative effect of greenhouse gases. *Philos. Trans. Roy. Soc. London*, **A360**, 1705–1719, doi:10.1098/rsta.2002.1027.

——, and Coauthors, 2011: Land use/land cover changes and climate: Modeling analysis and observational evidence. *Wiley Interdiscip. Rev. Climate Change*, **2**, 828–850, doi:10.1002/wcc.144.

Pitman, A. J., and Coauthors, 2009: Uncertainties in climate responses to past land cover change: First results from the LUCID intercomparison study. *Geophys. Res. Lett.*, **36**, L14814, doi:10.1029/2009GL039076.

Pleim, J. E., and A. Xiu, 2003: Development of a land surface model. Part II: Data assimilation. *J. Appl. Meteor.*, **42**, 1811–1822, doi:10.1175/1520-0450(2003)042<1811:DOALSM>2.0.CO;2.

Portmann, R. W., S. Solomon, and G. C. Hegerl, 2009: Spatial and seasonal patterns in climate change, temperatures, and precipitation across the United States. *Proc. Natl. Acad. Sci. USA*, **106**, 7324–7329, doi:10.1073/pnas.0808533106.

Prestemon, J. P., and R. C. Abt, 2002: Southern forest resource assessment highlights: The southern timber market to 2040. *J. For.*, **100**, 16–22.

Price, C. V., N. Nakagaki, K. J. Hit, and R. M. Clawges, 2007: Enhanced historical land-use and land-cover data sets of the U.S. Geological Survey. USGS Data Series 240. [Available online at http://pubs.usgs.gov/ds/2006/240/.]

Puma, M. J., and B. I. Cook, 2010: Effects of irrigation on global climate during the 20th century. *J. Geophys. Res.*, **115**, D16120, doi:10.1029/2010JD014122.

Rahmstorf, S., J. E. Box, G. Feulner, M. E. Mann, A. Robinson, S. Rutherford, and E. J. Schaffernicht, 2015: Exceptional twentieth-century slowdown in Atlantic Ocean overturning circulation. *Nat. Climate Change*, **5**, 475–480, doi:10.1038/nclimate2554.

Robinson, W. A., 2002: General circulation model simulations of recent cooling in the east-central United States. *J. Geophys. Res.*, **107**, 4748, doi:10.1029/2001JD001577.

Rodionov, S. N., 2004: A sequential algorithm for testing climate regime shifts. *Geophys. Res. Lett.*, **31**, L09204, doi:10.1029/2004GL019448.

Rogers, J. C., 2013: The 20th century cooling trend over the southeastern United States. *Climate Dyn.*, **40**, 341–352, doi:10.1007/s00382-012-1437-6.

Sau, F., K. J. Boote, W. M. Bostick, J. W. Jones, and M. I. Mínguez, 2004: Testing and improving evapotranspiration and soil water balance of the DSSAT crop models. *Agron. J.*, **96**, 1243–1257, doi:10.2134/agronj2004.1243.

Saxena, V. K., and S. Yu, 1998: Searching for a regional fingerprint of aerosol radiative forcing in the southeastern US. *Geophys. Res. Lett.*, **25**, 2833–2836, doi:10.1029/98GL02106.

Shi, W., F. Tao, and J. Liu, 2014: Regional temperature change over the Huang-Huai-Hai Plain of China: The roles of irrigation versus urbanization. *Int. J. Climatol.*, **34**, 1181–1195, doi:10.1002/joc.3755.

Steyaert, L. T., and R. G. Knox, 2008: Reconstructed historical land cover and biophysical parameters for studies of land-atmosphere interactions within the eastern United States. *J. Geophys. Res.*, **113**, D02101, doi:10.1029/2006JD008277.

Trail, M., A. P. Tsimpidi, P. Liu, K. Tsigaridis, Y. Hu, A. Nenes, B. Stone, and A. G. Russell, 2013: Potential impact of land use change on future regional climate in the southeastern U.S.: Reforestation and crop land conversion. *J. Geophys. Res. Atmos.*, **118**, 11 577–11 588, doi:10.1002/2013JD020356.

Vose, R. S., and Coauthors, 2014: Improved historical temperature and precipitation time series for U.S. climate divisions. *J. Appl. Meteor. Climatol.*, **53**, 1232–1251, doi:10.1175/JAMC-D-13-0248.1.

Waisanen, P. J., and N. B. Bliss, 2002: Changes in population and agricultural land in conterminous United States counties, 1790 to 1997. *Global Biogeochem. Cycles*, **16**, 1137, doi:10.1029/2001GB001843.

Wang, H., S. Schubert, M. Suarez, J. Chen, M. Hoerling, A. Kumar, and P. Pegion, 2009: Attribution of the seasonality and regionality in climate trends over the United States during 1950–2000. *J. Climate*, **22**, 2571–2590, doi:10.1175/2008JCLI2359.1.

Wang, Z., and Coauthors, 2014: Evaluation of MODIS albedo product (MCD43A) over grassland, agriculture and forest surface types during dormant and snow-covered periods. *Remote Sens. Environ.*, **140**, 60–77, doi:10.1016/j.rse.2013.08.025.

Wetzel, P. J., and J.-T. Chang, 1987: Concerning the relationship between evapotranspiration and soil moisture. *J. Climate Appl. Meteor.*, **26**, 18–27, doi:10.1175/1520-0450(1987)026<0018:CTRBEA>2.0.CO;2.

Wickham, J. D., T. G. Wade, and K. H. Riitters, 2012: Comparison of cropland and forest surface temperatures across the conterminous United States. *Agric. For. Meteor.*, **166–167**, 137–143, doi:10.1016/j.agrformet.2012.07.002.

——, ——, and ——, 2014: An isoline separating relatively warm from relatively cool wintertime forest surface temperatures for the southeastern United States. *Global Planet. Change*, **120**, 46–53, doi:10.1016/j.gloplacha.2014.05.012.

Wild, M., A. Ohmura, and K. Makowski, 2007: Impact of global dimming and brightening on global warming. *Geophys. Res. Lett.*, **34**, L04702, doi:10.1029/2006GL028031.

Yang, Z.-L., Y. Dai, R. E. Dickinson, and W. J. Shuttleworth, 1999: Sensitivity of ground heat flux to vegetation cover fraction and leaf area index. *J. Geophys. Res.*, **104**, 19 505–19 514, doi:10.1029/1999JD900230.

Yu, S., and Coauthors, 2014: Attribution of the United States "warming hole": Aerosol indirect effect and precipitable water vapor. *Sci. Rep.*, **4**, 6929, doi:10.1038/srep06929.

Zhang, X., L. A. Vincent, W. D. Hogg, and A. Niitsoo, 2000: Temperature and precipitation trends in Canada during the 20th century. *Atmos.–Ocean*, **38**, 395–429, doi:10.1080/07055900.2000.9649654.

Earth Interactions is published jointly by the American Meteorological Society, the American Geophysical Union, and the Association of American Geographers. Permission to use figures, tables, and *brief* excerpts from this journal in scientific and educational works is hereby granted provided that the source is acknowledged. Any use of material in this journal that is determined to be "fair use" under Section 107 or that satisfies the conditions specified in Section 108 of the U.S. Copyright Law (17 USC, as revised by P.IL. 94-553) does not require the publishers' permission. For permission for any other from of copying, contact one of the copublishing societies.